VOL. 11, NO. 3, FEBRUARY 2016 ISSN 1819-6608
ARPN Journal of Engineering and Applied Sciences

www.arpnjournals.com

EFFICIENCY IMPROVEMENT IN DUAL INVERTER FED OPEN-END PERMANENT MAGNET SYNCHRONOUS MOTOR

P. Archana[1] and K. Preetha[2]
[1]Power Electronics and Drives, DSEC, Perambalur, Tamil Nadu, India
[2]Department of Electrical and Electronics Engineering, DSEC, Perambalur, Tamil Nadu, India

ABSTRACT

Permanent magnet synchronous motor (PMSM) system and proposes control method which can generate maximum output power in overall speed range for integrated starter/alternator. This project analyzes the dual inverter driven open-end machine system consists of two inverters which are connected to the both ends of the machine winding. By disconnecting one inverter from the power source, the dc-link voltage of flying capacitor can be boosted through the machine. Because one inverter is connected to the only power source, output power of the machine is regulated by the source connected inverter. In this paper, modulation method for maximizing output power of inverter and motor with reduced harmonic and loss is proposed. It is a hybrid modulation combining seven-step and fast space vector pulse width modulations. With proposed method, efficiency and operation area are improved and cost of entire driving system is also decreased due to the removing of dc–dc converter. Analyses, strategies, control method, and simulation results are descripted. The experiments with PMSM are accomplished to verify the feasibility of proposed method.

Index terms: dual inverter, harmonic reduction, integrated starter/alternator (ISA), open-end winding, permanent magnet synchronous motor (PMSM) drive.

INTRODUCTION

Recently, because of the environmental problem and soaring of the fuel price, electric motor systems are adopted to the many kinds of traction applications such as train and vehicle which were traditionally driven by internal combustion engine (ICE) or external combustion engine (ECE). In addition, because efficiency of the electric traction system is higher than that of ICE, electric traction vehicles have higher mileage than the ICE vehicles. It is expected that efficiency of the future hybrid electric vehicle (HEV) and electric vehicle (EV) becomes higher than the current level thanks to the improvements of the inverter topology, switching devices, and motor design technologies.

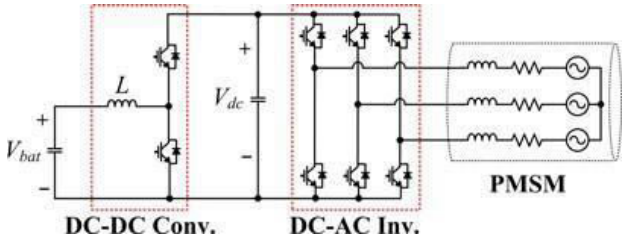

Figure-1. PMSM drive with dc–dc converter.

AC motors, permanent magnet synchronous motors (PMSMs), and induction motors, are generally used as traction motor for HEV due to their high efficiency although complex control technique is required. Among the ac motors, PMSMs are mostly used in HEV because of their high efficiency and compactness. Especially, interior permanent magnet synchronous motor (IPMSM) is suitable for HEV application due to its reluctance torques in field weakening region. Because the required operating region of HEV motor is much wider than that of other applications, the reluctance torque and wide field weakening characteristic make IPMSM adopted for traction motor of EV. The high efficiency of PMSM mainly comes from its inherent rotor flux from permanent magnet, whereas other motors need the rotor current for generating the rotor flux. Thanks to this rotor flux, efficiency below the rated speed is higher than other motors and the power factor of the PMSM is also higher than that of other machines. However, this constant rotor flux generates high back-electromotive force (back- EMF) in the high speed region. Because output voltage of the inverter should be controlled under the available range, field weakening control is necessary for the high speed operation. The negative d-axis current reduces back-EMF and lowers the required voltage.

Thus, system can be maintained in the stable operation. Although IPMSM shows higher efficiency than that of other PMSMs in high speed region, it is true that field weakening current restricts output torque and drops the efficiency. By these reasons, high dc-link voltage is required to reduce the field weakening current and secure the high speed operation of HEV. However, it is hard to make high dc-link voltage directly from the battery because stacking of battery cells requires complex cell balancing circuits. Most of all, high battery voltage is potentially dangerous. So, dc–dc boost converter is generally used to make high dc-link voltage from relatively low battery voltage.

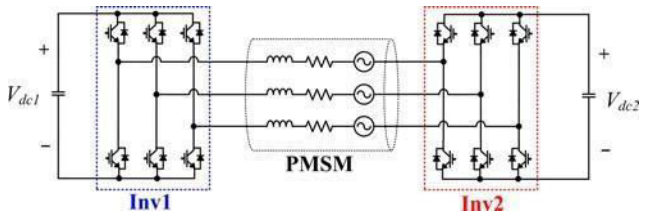

Figure-2. PMSM drive with dual inverter with flying inverter.

The simple schematic of drive system with such dc- dc converter. This kind of cascaded system, however, deteriorates the system efficiency. The boosting ratio of dc–dc converter is also not high, normally between 2 and 3, because high boosting ratio lowers efficiency. Because inductor used in dc–dc converter takes huge volume and weight, it is also pointed out as a drawback of dc–dc converter.

To overcome the demerits of the cascaded system with the dc–dc converter, several studies have been conducted. Z-source inverter proposed by Peng et al. is one of those studies. Z-source inverter uses no dc–dc converter and makes circuit simpler with inductors and capacitors. It also has a strong fault tolerance because it removes dead time between upper and lower switch. However, it is far from reducing the volume and weight because it requires two inductors and capacitors. The boosting ratio is also restricted by output voltage and shoot-through zero state. In, the cascaded H-bridge with flying capacitor is proposed to obtain higher output voltage. This method, however, requires not only many switches but also the complicated lookup table. The modulation index (MI) is also limited by the load condition.

BASICS OF OPERATION

The dual inverter system with flying capacitor satisfies the two main objects: load power regulation and flying dc-link voltage regulation. The former is for following the user command and the latter is for safe operation of the isolated inverter with flying capacitor. This section describes the control method satisfying the objects in the dual inverter with flying capacitor topology. Such an objective can be accomplished with voltage decoupling control proposed. The constraints of the proposed system and the advantages of dual inverter topology with flying capacitor are described in this section.

A. System modeling

In analyzing the modulation method and power flow, the electrical model of PMSM and dual inverter is considered. Figure-3 shows the electrical schematic of dual inverter and PMSM. PMSM is simply modeled with inductor, resistor, and back- EMF from electromagnetic coupling. The open stator windings are connected to the legs of *Inv*1 and Inv2.Inv1 connected to the battery is drawn at the left side of Figure-3 and *Inv*2 connected to the capacitor bank is at the opposite end. Terminals and switches of the *Inv*2 are expressed with prime for easy contrast.

Pole voltages of *Inv*1 are V_{ao}, V_{bo}, and V_{co}, and pole voltages of *Inv*2 are $V_{a'o'}$, $V_{b'o'}$, and $V_{c'o'}$. Phase voltages applied to the motor are expressed as

$$\begin{aligned} V_{aa'} &= V_{ao} - V_{a'o'} + V_{oo'} \\ V_{bb'} &= V_{bo} - V_{b'o'} + V_{oo'} \\ V_{cc'} &= V_{co} - V_{c'o'} + V_{oo'} \end{aligned} \quad (1)$$

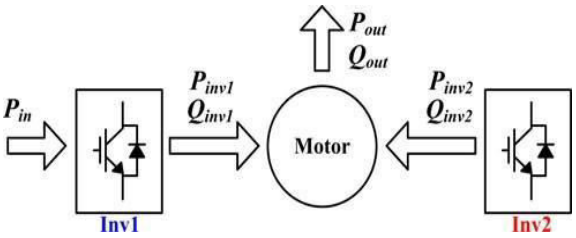

Figure-3. Power flow diagram of dual inverter system.

where the common mode voltage between both inverters, $V_{oo'}$, is defined as

$$V_{oo'} = (V_{ao}+V_{bo}+V_{co})/3 - (V_{ao'}+V_{bo'}+V_{co'})/3. \quad (2)$$

This common mode voltage does not contribute to the torque generation because only differential components generate torque. In the rotating reference frame, voltage to the motor can also be written as

$$\begin{aligned} V_d &= V_{d,\,inv1} - V_{d,\,inv2} \\ V_q &= V_{q,inv1} - V_{q,inv2} \end{aligned} \quad (3)$$

where V_d and V_q are the *d–q* stator voltages in the synchronous reference frame rotating at the angular velocity ω_r. $V_{d,inv1}$ and $V_{q,inv1}$ are the *d–q* output voltages of *Inv*1 and $V_{d,inv2}$ and $V_{q,inv2}$ are the *d–q* output voltages of *Inv*2 in the synchronous reference frame, respectively.

The voltage and torque equations for PMSM in the syn- chronous reference frame are written as

$$V_d = R_s I_d + pL_d I_d - \omega_r L_q I_q \quad (4)$$

$$V_q = R_s I_q + pL_q I_q + \omega_r (\lambda_f + L_d I_d) \quad (5)$$

$$T_e = \frac{3}{2}\frac{n_p}{2}[\lambda_f + (L_d - L_q) I_d] I_q \quad (6)$$

where I_d and I_q are the *d–q* stator currents in the synchronous reference frame. Resistance and inductances of the stator are denoted as R_s, L_d, and L_q. *p* indicates differential operator (d/dt), λf is rotor flux, and np is number of the poles.

B. Dual inverter with permanent magnet synchronous motor

The basic permanent magnet synchronous motor of proposed hybrid electrical vehicle is shown in Figure-4. Dual inverter is an electronic device or circuit made by the combination of two bridges. One of them works as rectifier and other bridge works as inverter. Thus an electronic circuit, in which two processes take place at same time, is known as dual converter. In three phase dual inverter, we make use of 3phase rectifier which converts 3 phase ac supply to dc. The rest of the process is same and same elements are used. The output of three phase rectifier is fed to filter and after filtering the pure dc fed to load. At last the supply from load is given to last bridge that is inverter. It do the inverter process of rectifier and converts dc into 3 phase ac which appears at output.

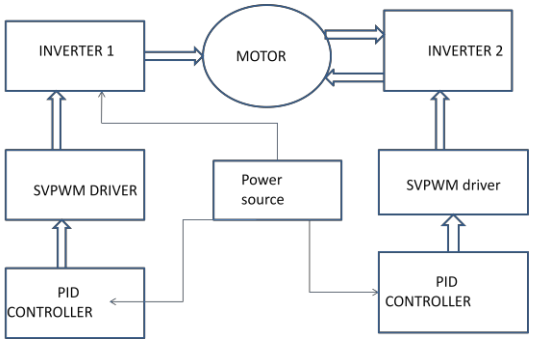

Figure-4. Block diagram.

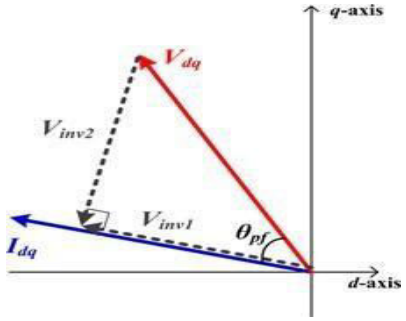

Figure-5. Vector diagram of current and decoupled voltage.

Reactive power is irrelevant to the flying dc-link voltage. Because input and output active powers only change dc- link voltage. This is common idea for the isolated power systems as in the static synchronous compensator (STATCOM) [36]. It can be summarized as

$$P_{inv2} = 0. \quad (7)$$

Because P_{out} and Q_{out} are regulated by motor controller, the following equations can be induced from (7) in ideal lossless system

$$P_{in} = P_{inv1} = P_{out} \quad (8)$$

$$Q_{inv1} + Q_{inv2} = Q_{out}. \quad (9)$$

C. Power control

Currents flowing in the system are identical in inverters and motor. Thus, output powers of the each component are varied with output voltages of inverters. $P_{in\ v\ 2}$ becomes zero when the amplitude of output voltage of the *Inv2*, $V_{in\ v\ 2}$, is zero or the angle difference between current and $V_{in\ v\ 2}$ is 90°.

Figure-3 demonstrates the power flow diagram of dual inverter with flying capacitor system. P and Q indicate the active and reactive powers, respectively. The subscripts indicate the power source. P_{in} shows the input power to the system and P_{out} and Q_{out} show the active and reactive powers consumed by the machine.

As aforementioned, main objects of the machine drive system by dual inverter with flying capacitor system is torques or speed regulation of the machine and flying dc- link voltage regulation. To accomplish the first object, P_{out} and Q_{out} are regulated. And the active power flow of the *Inv2*, $P_{in\ v\ 2}$, is controlled to zero in order to accomplish the second object.

At the same time, reactive power of the inv 1, Qinv1, should be controlled to zero to maximize the output active power because the apparent output power is limited by dc-link voltage connected to the power source when the constant current flows. Therefore, the reactive powers are controlled as

$$Qinv1=0 \quad (10)$$

$$Qinv2=Qout \quad (11)$$

Equation (10) and (11) indicates that the reactive power required to the motor is supplied by flying inverter. In other words, flying inverter works as a reactive power source.

D. Powers and voltages

In the conventional control method, output voltages of the components are determined to satisfy the aforementioned conditions [31], [32]. The previous researches give the ideas of making two output voltages orthogonal to maximize the output power while decoupling the power. Figure-5 shows the vector diagram of TABLE-1.

MODULATION INDICES

The conventional control method. By putting the output voltage Vector of the $V_{in\ v\ 1}$ in parallel with the current vector, it is possible to maximize the $P_{in\ v\ 1}$.

MODULATION METHOD

MI amplitude of first harmonics

Simultaneously, $V_{in\ v\ 2}$ is decided to orthogonal to the current vector to eliminate the active power flow to Inv2. Thus, (7), (8), and (10) are satisfied regardless of the operation condition.

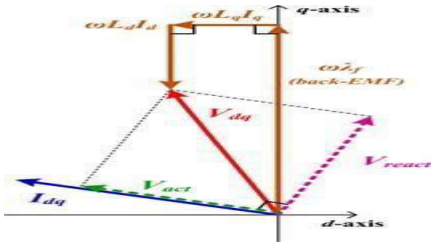

Figure-6. Vector diagram of IPMSM in high speed region.

In the case of the general machine drive system using only one inverter, the required power from the machine is entirely supplied by the single inverter. For the dual inverter with flying capacitor system, however, source connected inverter only takes charge of not the apparent power but the real power. Thus, constant active power can be supplied irrespective of load condition, while flying capacitor supplies reactive power. In summary, active output power in the low power factor region can be increased in the dual inverter system with flying capacitor.

General PMSM shows relatively high power factor at low speed and around the rated speed. Thus, the required reactive power is also not high. For the high speed region, however, negative d-axis current is definitely necessary to reduce the back- EMF induced by the rotor permanent magnets. Figure-6 shows the current and voltage vectors of IPMSM in high speed region. Thus, the reactive voltage is also high as much as the active voltage, Vact. The faster the machine rotates, the higher reactive voltage is required. Existence of the flying inverter and capacitor lightens the burden of reactive power and helps the efficient high speed drive.

Hybrid modulation of dual inverter with flying capacitor

In this section, power enhancement method using six- step modulation is proposed. Principle of operation is explained by comparing the proposed method with the conventional methods. This section also includes the analyses of proposed six- step modulation of dual inverter with flying capacitor scheme focusing on the power and voltage. To widen the operation of hybrid modulation method, phase shifting of six-step modulation method is also proposed. Field weakening control method which is essential for the high speed operation for the proposed modulation method is also suggested in this section.

SPWM	0.7854	$0.5\ V_{dc}$
Fast SVPWM	0.9067	$1/3\ V_{dc}$

A. Principle and objectives

Seven-step modulation is widely known as a modulation method which can generate maximum output voltage. Table-1 shows the maximum output voltage of the three representative modulation methods; sinusoidal PWM (SPWM), space vector PWM (SVPWM), and seven-step modulation. Seven-step modulation shows approximately 10% higher output voltage than SVPWM method. In addition, the switching loss also reduced, because only one switching is required in a period. Although the Seven - step modulation maximizes the amplitude of fundamental frequency component, it generates odd harmonics which lower the efficiency and cause the torque ripple and noise. It is also hard to apply to the machine which has small inductance because of the instant current soaring. Thus, it is temporarily used in dynamic situation such as rapid acceleration or the applications where the above defects are acceptable.

For the dual inverter topology, the voltage applied to the load is decided as a difference of the voltages from two inverters. Thus, the output voltage of the one inverter does not directly affect the load. This characteristic enables the hybrid modulation of dual inverter topology. In the proposed hybrid modulation method, input side inverter modulates the output voltage with seven -step. At the same time, opposite inverter compensates the odd harmonics generated from input side inverter. Thanks to the compensation of the flying inverter, load voltage, and current are maintained in sinusoidal form without harmonics. In summary, proposed method takes advantages of the Seven -step modulation such as low switching loss and high output power and removes the disadvantages such as high order harmonics and torque ripple.

The hybrid modulation suggested in [28] and [29] uses the same characteristics of the dual inverter topology. However, the huge battery bank is hard to apply to the flying dc-link capacitor in the motor drive application. Furthermore, the battery bank also can be recognized as isolated power source not a small dc-link capacitor. Because the six-step modulation generates fluctuating active power, voltage of the small dc-link capacitor also fluctuates. Thus, the ripple power from the Seven -step operation need to be analyzed and it is accomplished in the following section.

B. fast space vector modulation

The fast SVPWM based techniques is useful in systems with or without neutrality, unbalanced load, and triple harmonics, as well as for generating 3D control vector Dwell time calculation and switching sequence generation for the selected two-level hexagon can be performed in a manner similar to that in the conventional two-level SVPWM technique. Each two-level hexagon is divided into six sectors. The sector in reference vector Vrefo2 depends on its angle θo2.Vrefo2 can then be synthesized by the three stationary vectors of that sector. Dwell time calculation for the stationary vectors is performed based on the "volt-second-balancing" principle. The outer region two-level Hexagon OH1and

reference voltage Vrefo2 VectorsV1 (P2N2N2), V2 (P2N1N2) and P2N1N1, P2N2N2 is zero voltage vectorsV0. The volt-second-balancing equation for this sector is given as follows: Vrefo2Ts= V1Ta+ V2Tb+ V0T0, (5) where Ts is the sampling interval; and Ta, Tb, andT0 are the respective dwell times for vectors V1, V2, and V0. The values of Ta, Tb, and T0 are given as follows:

Ta = Ts×ma Sin (Π − θ), (6) Tb = Ts×maSin θ, (7) To = Ts - Ta−Tb, (8) where ma is the modulation index defined as follows: Ma= √3 Vref. (9) After calculating dwell time intervals, an appropriate design for the switching sequence is required. The typical seven-segment switching sequence is used in this scheme. The switching sequence should be designed, such that a change from one switching state to the next involves only one leg, and a change from one sector to the next involves zero or a minimum number of switching With these constraints, the seven-segment switching sequence for vector Vrefo2 is given as follows: (P1N2N2), (P2N2N2), (P2N1N2),(P2N1N1),(P2N1N2), (P2N2N2), (P1N2N2). Similarly, the switching sequence for Sector II is given as follows: (P1N2N2), (P2N2N2), (P2N1N2), (P2N1N1), (P2N1N2), (P2N2N2), (P1N2N2). This technique further reduces the number of two-level hexagons that should be considered. Consequently, it decreases the complexity and efforts involved in the SVPWM of a inverter. The fast SVPWM for this technique is initially resolved into inner and outer regions, similar to in the OSVPWM technique. Thus, the number of two-level hexagons that should be considered for the FOSVPWM of a five-level inverter is reduced to 18. The modulation index Ma for SVM is defined as the maximum value (Ma = 1) that corresponds to the radius of the largest circle that can be inscribed in the SVD.

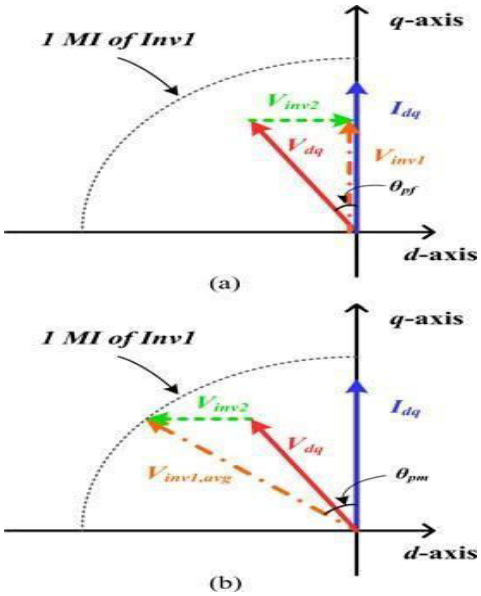

Figure-7. Vector diagrams of dual inverter system at low speed region. (a) In-phase modulation. (b) Phase shift modulation.

This paper proposes a phase modulation to solve these problems. The phase modulation methodswas widely researched for high speed dc–dc conversion circuit such as dual active bridge [39], [40], and phase shift converter [41]. Similar to these methods, it is possible to adjust the power in the dual inverter system using phase modulation method. Figure-7 shows the vector diagrams of the average voltage and current in synchronous reference frame. In the conventional method, output voltages of the two inverters are decided orthogonally to decouple the power as shown in the Figure-7(a). In this case, however, amplitude of the $V_{in\ v\ 1}$ becomes lower than the unity MI and should be chopped by switching. For the six-step phase modulation method, amplitude of the $V_{in\ v\ 1}$ is fixed to unity MI as represented in Figure-7(b). By replacing the current angle to the average voltage angle, from θ_i to $\theta_i + \theta_{pm}$, where θ_{pm} is the phase modulation angle defined as the phase difference between current and modulated $V_{in\ v\ 1}$. For example, when the θ_{pm} is 40° and θ_i is 5°, $V_{in\ v\ 1}$ is decided to vertex no. 2. If the θ_{pm} is 40° and θ_i is −20°, $V_{in\ v\ 1}$ is located on vertex no. 1. Phase modulated voltage $V_{in\ v\ 1,avg}$ is decided to transfer same amount of active power to the system. Thus, the average active component of the $V_{in\ v\ 2}$ becomes zero.

The active component voltage from inv1 can be mathematized as

$$V_{inv1,act}=2/\pi V_{dc1}\cos\Theta_{pm} \quad (12)$$

Where θ_{pm} is the most important value for the phase modulation method and can be obtained with current reference and active voltage as

$$\Theta_{pm}=\cos^{-1}(V_{act}/2/\pi V_{dc1}) \quad (13)$$

Because two solutions for (20) always exist, the selection pro- cedure for the optimal solution is required. Both solutions give the same active voltage but the amplitudes of reactive voltages generated by seven-step are different each other. By selecting the optimal θ_{pm}, it is possible to moderate the compensation burden of the *Inv*2. Because V_{dc2} can be controlled with the lower value with this properly selected θ_{pm}, the inverter loss can be reduced. The optimal value of θ_{pm} can be acquired by comparing it with θ_{pf}. choosing θ_{pm} which has same sign with θ_{pf} gives optimal θ_{pm} that can minimizes the reactive voltage for the *Inv*2.

D. Field weakening control

High speed operation is the main purpose of the dual inverter with flying capacitor system and it cannot be operated without the field weakening control methods have been suggested for several decades [1]-[8]. Among them, this paper introduces the voltage feedback method only because it is free from the load parameters and simple to apply [8]. This method just feeds the output voltage reference back and regulates it by lowering d-

axis current. The biggest difference between the field weakening control of single inverter system and that of dual inverter with flying capacitor system is the voltage which is fed back.

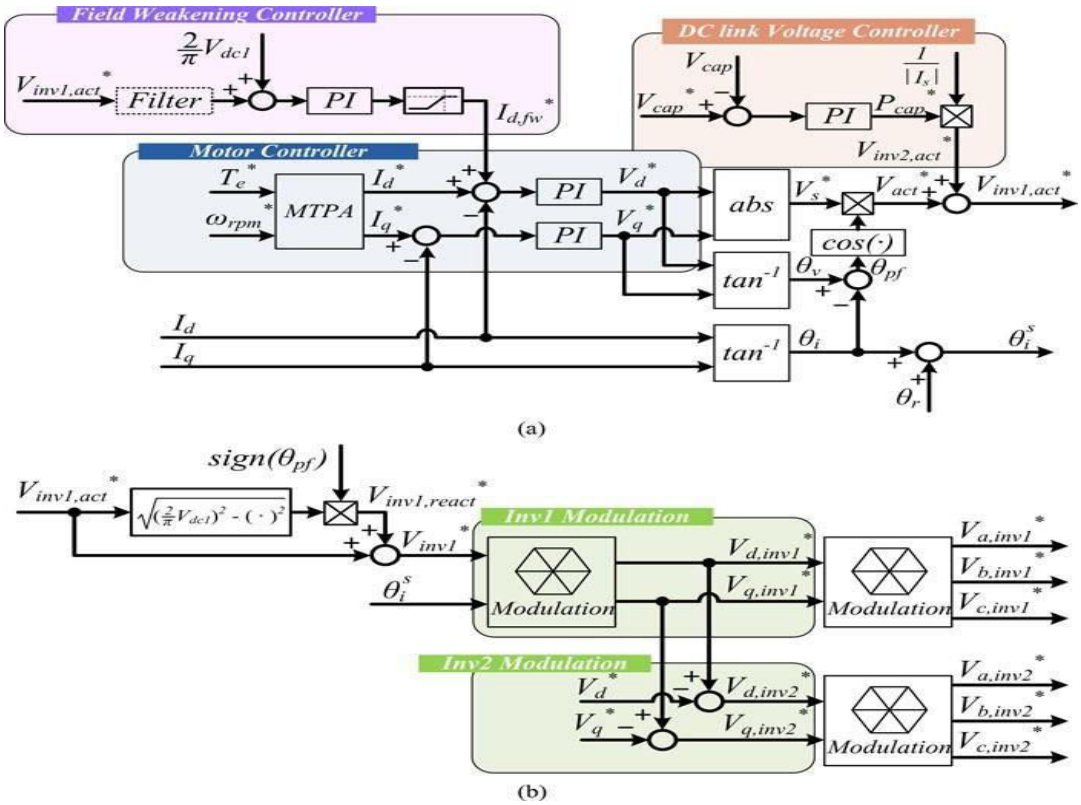

Figure-8. Configuration of controller for seven-step modulation of dual inverter with flying inverter. (a) Motor, field weakening, and dc-link voltage controller. (b) Phase modulator and voltage modulation stage.

The field weakening control generally used for the single inverter system regulates the output reference voltage to the linear range. For the dynamic performance and the control stability, the voltage limit is set to have 5%–10% margin. Thus, the voltage limit becomes (26) when SVPWM is applied

$$Vlim = \eta V\sqrt{dc}/3 \quad (14)$$

where η is voltage margin coefficient which generally has value around 0.9–0.95. In the previous studies, this limited voltage is applied to the dual inverter system and limits output voltage. This marginal voltage can be considered as a wasted voltage. For the dual inverter system with six step modulation, the voltage limit goes up to 1 MI regardless of margin and the voltage limit can be written as (27)

$$Vlim=2/\pi Vdc1. \quad (15)$$

Thus, the voltage wasted for the margin can be eliminated. This output voltage maximization minimizes field weakening current and improves system efficiency. Furthermore, the increment is not the apparent power but the pure active power. Therefore, this increment effect is not negligible. The active voltage reference for the *Inv*1 includes the active voltage for the load and *V*dc2 regulation. Whereas the active voltage for the load becomes constant in steady state, the active voltage required for regulating *V*dc2 fluctuates due to the seven-step operation. For this reason, the *d*-axis current also becomes fluctuating. The fluctuating current generates errors in controller.

Thus, this fluctuating component should be minimized for stable operation. It can be reduced by lowering the cut-off frequency of the field weakening controller. This method, however, also lowers the dynamic performance of the system such as acceleration, deceleration, and *V*dc2 regulation. Because fluctuating voltage of *V*dc2 is mainly composed of six times of rotating frequency, it also can be filtered by low pass or notch filter. This method can lessen the current fluctuation while it maintains the dynamic performance.

E. System control

*The controller of the proposed seven-step modulation for *d* dual inverter with flying capacitor is composed as shown in Figure-16. Figure-16(a) shows the motor controller, field weakening controller, and flying dc-link voltage controller and Figure-16(b) shows the voltage modulation stage. Motor controller part is quite similar with the conventional motor controller. It is composed of MTPA table or algorithm and two PI current regulators which control d–q axis currents in the

synchronous reference frame. Output active voltage required to the motor is calculated ith the outputs of the two current regulators, Vd^* and V_q*. DC-link voltage controller is also necessary to control the flying dc-link voltage. It is simply composed of one PI regulator. It gives the power required to the flying dc link and it is converted to the active voltage reference $Vin\ v\ 2, ac\ t^*$. Two active voltage references are added and become the active voltage reference of the Inv1. Phase modulation algorithm is applied after calculating $Vin\ v\ 1, ac\ t^*$ and gives the reactive voltage reference $Vin\ v\ 1, re\ a\ c\ t^*$.

The output voltage references are modulated with seven- step for Inv1. The current angle and rotor position are required to convert voltages and currents between d–q components and active/reactive components. The field weakening controller also gives d-axis current reference.

Field weakening current controller regulates $Vin\ v\ 1\ ac\ t^*$ to 1 MI. This controller can contain low pass filter or notch filter for the better performance.

EXPERIMENTAL RESULTS

To verify the validity of the proposed control method, experiments are accomplished with a PMSM. 148 constant value are given to PID controller and we get the output voltage of motor is 148. The peak value is Instead of battery dc power supply is simply adapted to the power source. Although the flying dc-link voltage can be controlled according to the operating condition, it is fixed to 148 v to compare efficiency. For inverter 1 and 2 dc bus voltage is 30v and snubber resistance is 1e5 ohms.

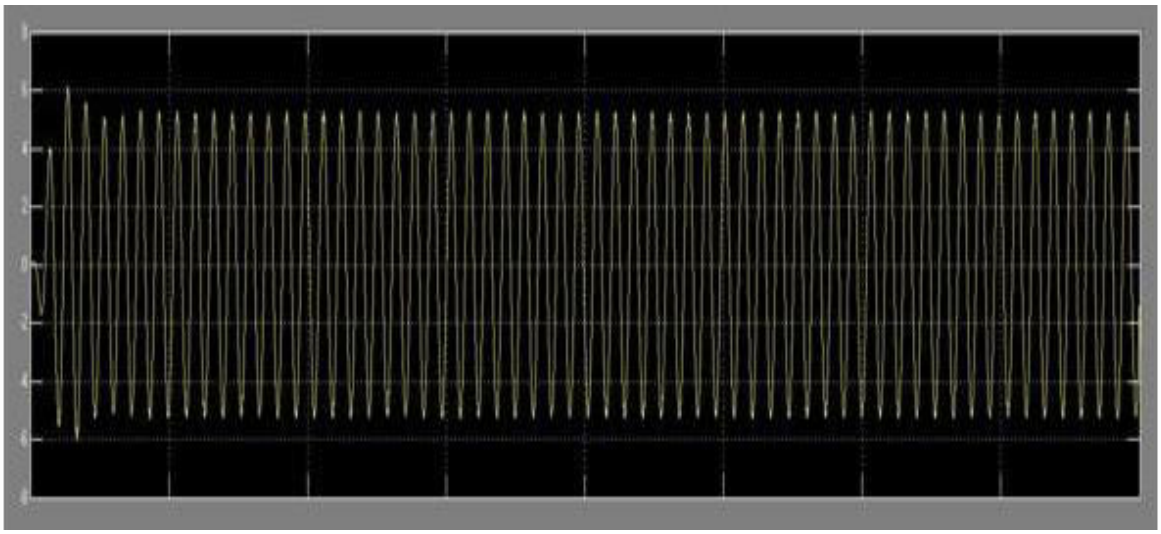

Figure-9. Fast SVPWM.

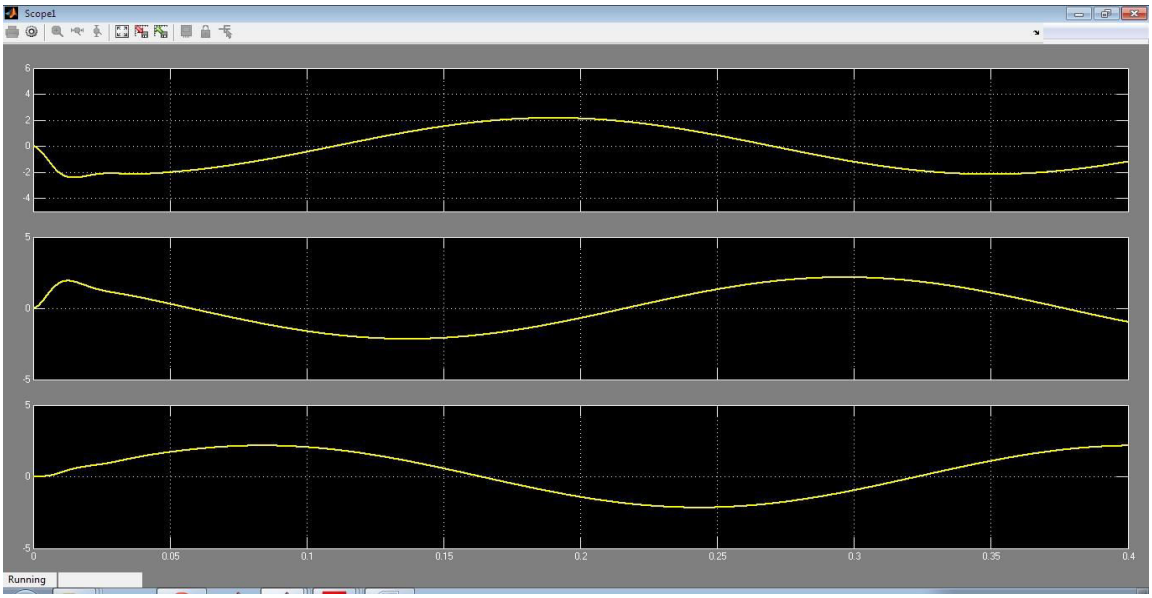

Figure-10. Motor current.

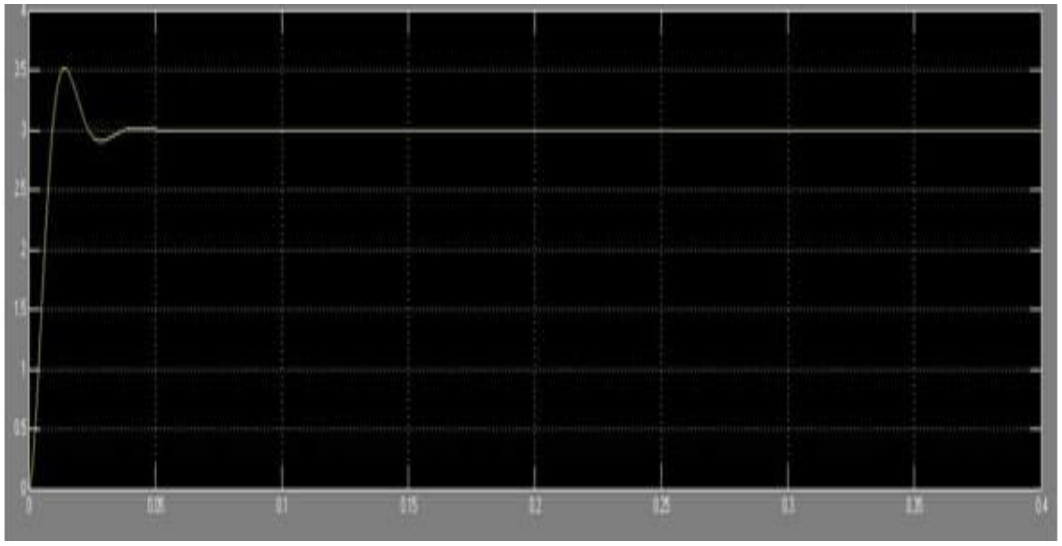

Figure-11. Motor torque.

Figure-12. Motor output voltage.

In fast svpwm resistance, Vdc and power value are constant that value is o.8 ohm, 310 v and 8.It definitely shows that current waveforms are pure sinusoidal for permanent magnet synchronous motor during hybrid modulation. It remarks that the torque ripples are not caused by the seven step operation of inv 1. The current ripples also can be minimized by adjusting Vdc2 in accordance with the operating condition.

Fig shows the experimentally achieved operation areas of the machine according to the three different driving methods. As verified in the previous researches of [31] and [32], operation area of the dual inverter with flying capacitor is much larger than that of the single inverter case.

CONCLUSIONS

This paper presents the hybrid modulation method which uses hybrid modulation which combines the seven-step modulation and fast SVPWM for dual inverter with flying capacitor topology. The proposed modulation method features the high efficiency and wide operation area. It maximizes the advantages of the dual inverter system and minimizes the defects such as battery current ripple and high inverter loss. The proposed method enlarges the seven-step operation area to the whole operation region including the low speed where the conventional method cannot operate. Thanks to the seven-step operation of the battery side inverter in whole operation region, the battery side dc-link filter can be reduced. This paper analyzes the modulation method especially considering the power flow between the inverter and motor. The field weakening method and controller for the proposed method are also presented. The reduced scale experiments with the PMSM are also executed to verify the superiority of the proposed method. The experimental results prove that the proposed method gives the high efficiency and large operation area.

REFERENCES

J.-K. Seok and S.-K. Sul. 1999. Optimal flux selection of an induction machine for maximum torque operation in flux-weakening region. IEEE Trans. Power Electron. vol. 14, no. 4, pp. 700–708, July.

M. Tursini, E. Chiricozzi, and R. Petrella. 2010. Feedforward flux-weakening control of aurface- mounted permanent-magnet synchronous motors accounting for resistive voltage drop. IEEE Trans. Ind. Electron. vol. 57, no. 1, pp. 440–448, January.

T.-S. Kwon and S.-K. Sul. 2006. Novel antiwindup of a current regulator of a surface-mounted permanent- magnet motor for flux-weakening control. IEEE Trans. Ind. Appl. vol. 42, no. 5, pp. 1293–1300, September/October.

S. Kim and J.-K. Seok. 2013. Maximum voltage utilization of IPMSMs using modulating voltage scalability for automotive applications. IEEE Trans. Power Electron. vol. 28, no. 12, pp. 5639–5646, December.

A. Tripathi, A. M. Khambadkone, and S. K. Panda. 2006. Dynamic control of torque in overmodulation and in the field weakening region. IEEE Trans. Power Electron. vol. 21, no. 4, pp. 1091–1098, July.

M. Mengoni, L. Zarri, A. Tani, G. Serra, and D. Casadei. 2012. A comparison of four robust control schemes for field-weakening operation of induction motors. IEEE Trans. Power Electron. vol. 27, no. 1, pp. 307–320, January.

H. Liu, Z.Q. Zhu, E. Mahamed,Y. Fu, and X. Qi. 2012. Flux-weakening control of nonsalient pole PMSM having large winding inductance, accounting for resistive voltage drop and inverter nonlinearities. IEEE Trans. Power Electron. vol. 27, no. 2, pp. 942–952, February.

J.-M. Kim and S.-K. Sul. 1997. Speed control of interior permanent magnet synchronous motor drive for the flux weakening operation. IEEE Trans.Ind. Appl. vol. 33, no. 1, pp. 43-48, January/February.

C.-H. Kim, M.-Y.Kim, H.-S. Park and G.-W. Moon. 2012. A modularized two stage charge equalizer with cell selection switches for series-connected lithium-ion battery string in an HEV. IEEE Trans. Power Electron. vol. 27, no. 8, pp. 3764–3774, August.

M. Einhorn,W. Roessler, and J. Fleig. 2011. Improved performance of serially connected Li-ion batteries with active cell balancing in electric vehicles. IEEE Trans. Veh. Technol. vol. 60, no. 6, pp. 2448–2457, July.

A. M. Imtiaz and F. H. Khan. 2013. Time shared flyback converter" based regenerative cell balancing technique for series connected Li-ion battery strings. IEEE Trans. Power Electron. vol. 28, no. 12, pp. 5960-5975, December.

S. J. Moura, J. L. Stein, and H. K. Fathy. 2013. Battery-health conscious power management in plug-in hybrid electric vehicles via electrochemical modelling and stochastic control. IEEE Trans. Contr. Syst. Technol. vol. 21, no. 3, pp. 679-694, May.

Z. Zheng, K. Wang, L. Xu, and Y. Li. 2014. A hybrid cascaded multilevel converter for battery energy management applied in electric vehicles. IEEE Trans. Power Electron. vol. 29, no. 7, pp. 3537–3546, July.

J. O. Estima and A. J. Marques Cardoso. 2012. Efficiency analysis of drive train topologies applied to electric/hybrid vehicles. IEEE Trans. Veh. Technol. vol. 61, no. 3, pp. 1021–1031, March.

Z. Du, B. Ozpineci, L. M. Tolbert, and J. N. Chiasson. 2009. DC–AC cascaded H-bridge multilevel boost inverter with no inductors for electric/hybrid electric vehicle applications. IEEE Trans. Ind. Appl. vol. 45, no. 3, pp. 963-970, May/June.

F. Z. Peng. 2003. Z-source inverter. IEEE Trans. Ind. Appl. vol. 39, no. 2, pp. 504–510, March/April.

M. Shen, A. Joseph, J. Wang, F. Z. Peng, and D. J. Adams. 2007. Comparison of traditional inverters and Z-source inverter for fuel cell vehicles. IEEE Trans. Power Electron. vol. 22, no. 4, pp. 1453–1463, July.

F. Guo, L. Fu, C.-H. Lin, C. Li, W. Choi, and J. Wang. 2013. Development of an 85-kw bidirectional quasi-Z- source inverter with DC-link feed-forward compensation for electric vehicle applications. IEEE Trans. Power Electron. vol. 28, no. 12, pp. 5477–5488, December.

O. Ellabban, J. V. Mierlo, and P. Lataire. 2012. A DSP-based dual-loop peak DC-link voltage control strategy of the Z-source inverter. IEEE Trans. Power Electron. vol. 27, no. 9, pp. 4088–4097, September.

K. R. Sekhar and S. Srinivas. 2013. Discontinuous decoupled PWMs for reduced current ripple in a dual two-level inverter fed open-end winding induction motor drive. IEEE Trans. Power Electron. vol. 28, no. 5, pp. 2493-2502, May.

V. T. Somasekhar, S. Srinivas, and K. K. Kumar. 2008. Effect of zero-vector placement in a dual-inverter fed open-end winding induction-motor drive with a decoupled space-vector PWM strategy. IEEE Trans. Ind. Electron. vol. 55, no. 6, pp. 2497–2505, June.

S. Srinivas and K. R. Sekhar. 2013. Theoretical and experimental analysis for current in a dual-inverter-fed open-end winding induction motor drive with reduced

switching PWM. IEEE Trans. Ind. Electron. vol. 60, no. 10, pp. 4318-4328, October.

V. T. Somasekhar, K. Gopakumar, M. R. Baiju, K. K. Mohapatra, and L. Umanand. 2005. A multilevel inverter system for an induction motor with open-end windings. IEEE Trans. Ind. Electron. vol. 52, no. 3, pp. 824-836, June.

V. T. Somasekhar, S. Srinivas, and K. K. Kumar. 2008. Effect of zero-vector placement in a dual-inverter fed open-end winding induction motor drive with alternate sub-hexagonal center PWM switching scheme. IEEE Trans. Power Electron. vol. 23, no. 3, pp. 1584–1591, May.

C. Patel, R. P. P. A. Day, A. Dey, R. Ramchand, K. Gopakumar, and M. P. Kazmierkowski. 2012. Fast direct torque control of and open-end induction motor drive using 12-sided polygonal voltage space vectors. IEEE Trans. Power Electron. vol. 27, no. 1, pp. 400–410, January.

Y. Wang, D. Panda, T. A. Lipo and D. Pan. 2013. Open-winding power conversion systems fed by half-controlled converters. IEEE Trans. Power Electron. vol. 28, no. 5, pp. 2427-2436, May.

M.-S. Kwak and S.-K. Sul. 2008. Control of an open-winding machine in a grid-connected distributed generation system. IEEE Trans. Ind. Appl. vol. 44, no. 4, pp. 1259-1267, July/August.

S. D. G. Jayasinghe, D. M. Vilathgamuwa, and U. K. Madawala. 2011. Direct integration of battery energy storage systems in distributed power generation. IEEE Trans. Energy Convers. vol. 26, no. 2, pp. 677-685, June.

S. D. G. Jayasinghe, D. M. Vilathgamuwa, and U. K. Madawala. 2013. A dual inverter-based supercapacitor direct integration scheme for wind energy conversion systems. IEEE Trans. Ind. Appl. vol. 49, no. 3, pp. 1023-1030, May/June.

J. Hong, H. Lee, and K. Nam. 2014. Charging method for the second battery in dual-inverter drive systems for electric vehicles. In: Proc. IEEE 29th Annu. Appl. Power Electron. Conf. Expo. March 16-20, pp. 2407–2414.

J. Kim, J. Jung, and K. Nam. 2004. Dual-Inverter control strategy for high speed operation of EV induction motors. IEEE Trans. Ind. Electron. vol. 51, no. 2, pp. 312-320, April.

D. Pan, F. Liang, Y. Wang, and T. A. Lipo. 2014. Extension of the operating region of an IPM motor utilizing series compensation. IEEE Trans. Ind. Appl. vol. 50, no. 1, pp. 539–548, January/February.

J. Ewanchuk, J. Salmon, and C. Chapelsky. 2013. A method for supply voltage boosting in an open-ended induction machine using a dual inverter system with a floating capacitor bridge. IEEE Trans. Power Electron. vol. 28, no. 3, pp. 1348-1357, March.

T. Gerrits, C. G. E. Wijnands, J. J. H. Paulides and J. L. Duarte. 2012. Dual voltage source inverter topology extending machine operating range. In: Proc. IEEE Energy Convers. Conf. Exhibit. September, pp. 2840-2846.

Y. Lee and J.-I. Ha. 2013. Power enhancement of dual inverter for open-end permanent magnet synchronous motor. In: Proc. IEEE Appl. Power Electron. Conf. Expo. March, pp. 1545-1551.

P. Rao, M. L. Crow, and Z. Yang. 2000. STATCOM control for power system voltage control applications. IEEE Trans. Power Del. vol. 15, no. 4, pp. 1311–1317, October.

P. D. Evans and R. J. Hill-Cottingham. 1986. DC link current in PWM inverters. IEEE Proc. B, vol. 133, no. 4, pp. 217–224, July.

M. Uno and K. Tanaka. 2011. Influence of high-frequency charge-discharge cycling induced by cell voltage equalizers on the life performance of lithium-ion cells. IEEE Trans. Veh. Technol. vol. 60, no. 4, pp. 1505-1515, May.

B. Zhao, Q. Song and W. Liu. 2012. Power characterization of isolated bidirectional dual-active-bridge DC–DC converter with dual-phase-shift control. IEEE Trans. Power Electron. vol. 27, no. 9, pp. 4172–4176, September.

H. Bai and C. Mi. 2008. Eliminate reactive power and increase system efficiency of isolated bidirectional dual-active-bridge DC-DC converters using novel dual-phase-shift control. IEEE Trans. Power Electron. vol. 23, no. 6, pp. 2905–2914, November.

Yongjae Lee, and Jung-Ik Ha. 2015. Hybrid Modulation of Dual Inverter for Open-End Permanent Magnet Synchronous Motor. IEEE Transactions on Power Electronics, Vol. 30, No. 6, June.

P. Satish Kumar, J. Amarnath and S.V.L. Narasimham. 2010. A Fast Space-Vector Pulse with Modulation Method for Diode-Clamped Multi-level Inverter fed Induction Motor. Asian Power Electronics Journal. Vol. 4 No.1 April.

I.-H. Cho, K.-M Cho, J.-W Kim, and G.-W. Moon. 2011. A new phase-shifted full-bridge converter with maximum duty operation for server power system. IEEE Trans. Power Electron. vol. 26, no. 12, pp. 3491–3500, December.